



Published in final edited form as:

Bone. 2018 July ; 112: 145–152. doi:10.1016/j.bone.2018.04.023.

Evaluation of Cross-Sectional and Longitudinal Changes in Volumetric Bone Mineral Density in Postmenopausal Women Using Single- versus Dual-Energy Quantitative Computed Tomography

Jad G. Sfeir, M.D.¹, Matthew T. Drake, M.D., Ph.D.¹, Elizabeth J. Atkinson, M.S.², Sara J. Achenbach, M.S.², Jon J. Camp, B.S.³, Amanda J. Tweed¹, Louise K. McCready, R.N.¹, Lifeng Yu, Ph.D.⁴, Mark C. Adkins, M.D.⁴, Shreyasee Amin, M.D., M.P.H.⁵, and Sundeep Khosla, M.D.¹

¹Robert and Arlene Kogod Center on Aging and Division of Endocrinology, Mayo Clinic, Rochester, MN 55905

²Department of Health Sciences Research, Mayo Clinic, Rochester, MN 55905

³Department of Physiology and Biomedical Engineering, Mayo Clinic, Rochester, MN 55905

⁴Department of Radiology, Mayo Clinic, Rochester, MN 55905

⁵Division of Rheumatology, Mayo Clinic, Rochester, MN 55905

Abstract

Central quantitative computed tomography (QCT) is increasingly used in clinical trials and practice to assess bone mass or strength and to evaluate longitudinal changes in response to drug treatment. Current studies utilize single-energy (SE) QCT scans, which may be confounded both by the amount of bone marrow fat at baseline and changes in marrow fat over time. However, the extent to which marrow fat changes either underestimate volumetric BMD (vBMD) measurements at baseline or under-/overestimate longitudinal changes *in vivo* in humans remains unclear. To address this issue, 197 early postmenopausal women [median age (IQR) 56.7 (54.4–58.7) years] underwent spine and hip QCT scans at baseline and 3 years using a 128-slice dual-source dual-energy (DE) scanner. The scans were analyzed as either SE scans (100 kVp) or DE scans (100 kVp and 140 kVp), with the latter accounting for bone marrow fat. At baseline, vertebral trabecular vBMD was (median) 17.6% lower ($P < 0.001$) while femur neck (FN) cortical vBMD was only 3.2% lower ($P < 0.001$) when assessed by SE vs DE scanning. SE scanning overestimated the 3 year rate of bone loss for trabecular bone at the spine by 24.2% ($P < 0.001$ vs DE rates of loss) but only by 8.8% for changes in FN cortical vBMD ($P < 0.001$ vs DE rates of

Corresponding author: Sundeep Khosla, MD, College of Medicine, Mayo Clinic, 200 First Street SW, Rochester, Minnesota 55905; khosla.sundeep@mayo.edu; Tel: 507-255-6663; Fax: 507-293-3853.

Disclosure statement: JJC and the Mayo Clinic have a financial interest in the software used to analyze the computed tomography scans.

Publisher's Disclaimer: This is a PDF file of an unedited manuscript that has been accepted for publication. As a service to our customers we are providing this early version of the manuscript. The manuscript will undergo copyediting, typesetting, and review of the resulting proof before it is published in its final citable form. Please note that during the production process errors may be discovered which could affect the content, and all legal disclaimers that apply to the journal pertain.

loss). The deviation between SE and DE rates of bone loss in trabecular vBMD became progressively greater as the rate of bone loss increased. These findings demonstrate that SE QCT scans underestimate trabecular vBMD and substantially overestimate rates of age-related bone loss due to ongoing conversion of red to yellow marrow. Further, the greater the rate of bone loss, the greater the overestimation of bone loss by SE scans. Although our findings are based on normal aging, recent evidence from animal studies demonstrates that the skeletal anabolic drugs teriparatide and romozosumab may markedly reduce marrow fat, perhaps accounting for the disproportionate increases in trabecular vBMD by SE QCT as compared to dual-energy x-ray absorptiometry with these agents. As such, future studies using recently available DE scanning technology that has satisfactory precision and radiation exposure are needed to evaluate changes in trabecular vBMD independent of changes in marrow fat with aging and drugs that may alter marrow fat composition.

Keywords

Menopause; osteoporosis; DXA; quantitative computed tomography

Introduction

In humans, bone marrow occupies about 85% of the bone cavity, with the remainder of the cavity consisting of trabecular bone.[1] During normal physiologic aging, as well as in various disease states, red hematopoietic marrow is progressively converted to yellow fatty marrow. Importantly, during the perimenopausal transition, a period characterized by rapid bone loss in women, changes in the amount of marrow fat can impact the assessment of bone mineral density (BMD) due to the fact that marrow fat has lower radiodensity relative to bone, thereby leading to underestimation of volumetric BMD (vBMD) using conventional single energy (SE) quantitative computed tomography (QCT) methods.

Central QCT has been increasingly employed in both clinical trials and practice to assess bone mass and strength and to evaluate longitudinal skeletal changes in response to pharmacologic intervention. Current studies utilize SE QCT scans which offer the advantages of 3-dimensional evaluation of bone structure and estimations of vBMD due to the ability of QCT to allow for the separate evaluation of cortical and trabecular compartments. The trabecular compartment is of particular importance due to its high metabolic activity and consequent susceptibility to changes in vBMD, but image assessment is highly influenced both by the degree of marrow fat at baseline and changes in marrow fat over time.[2, 3] It has long been recognized that accounting for marrow fat in the assessment of vBMD, using techniques such as dual energy (DE) QCT, provides a more accurate estimation of both bone mass and mineral content,[4, 5] although previous studies have been performed in cadaveric specimens and there is currently no data on longitudinal changes in DE QCT vBMD *in vivo* in humans. In particular, SE QCT scans have routinely been used for research and clinical purposes due to concerns regarding radiation exposure and increased variability of DE QCT scans.[4, 5]

Given these considerations, in this study we sought to quantify the underestimation of vBMD at the lumbar spine and femoral neck when assessed by SE QCT versus DE QCT as well as the potential overestimate of rates of bone loss by SE QCT during longitudinal 36-month follow-up imaging. For this comparison, we used DE QCT technology to assess postmenopausal bone loss in women independent of changes in marrow fat.

Methods

Study Subjects

We recruited 199 women aged 50–61 years between 2011 and 2012. The sample size was based on power calculations to provide 90% power to detect 0.8%/yr (and 80% power to detect 0.7%/yr) changes in lumbar spine trabecular vBMD using DE QCT in early postmenopausal women. In our previous studies, the average changes over 3 yrs in lumbar spine trabecular vBMD by SE QCT were 1.7%/yr in similar age women,[6] so we planned for a sample size that would allow as much as a 50% overestimation of rates of bone loss by SE versus DE QCT. Inclusion criteria were postmenopausal status (absence of menses for 1 year and serum FSH level > 20 IU/L) as well as total hip or lumbar spine BMD T-score between -1 and -2.5. Exclusion criteria included: 1) Total hip or lumbar spine BMD T-score at or below -2.5; 2) abnormality in any of the following screening laboratory studies: serum calcium, phosphorus, alkaline phosphatase, aspartate aminotransferase, or creatinine; 3) presence of significant liver or renal disease, malignancy, malabsorption syndrome, hypo- or hyperparathyroidism, acromegaly, Cushing's syndrome, hypopituitarism, or severe chronic obstructive pulmonary disease; 4) history of oral or inhaled corticosteroid use > 3 months, anticonvulsant therapy (within previous year), sodium fluoride (any history), pharmacological doses of thyroid hormone (causing decline of thyroid stimulating hormone below normal), or treatment within the past 3 years with bisphosphonates, denosumab, parathyroid hormone, calcitonin, strontium, estrogen, or a selective estrogen receptor modulator. Subjects with a clinical history of an osteoporotic fracture (spine, hip, or distal forearm) were also excluded. Of the 199 women enrolled in the study, we excluded two women from analyses who did not have valid baseline QCT data for either the femur neck or lumbar spine.

Study protocol

The protocol was approved by the Mayo Clinic Institutional Review Board and all studies were performed in the Mayo Clinic Clinical Research and Trials Unit (CRTU). Blood samples were obtained fasting at 8 am. Spine and hip DXA measurements were obtained using a Lunar Prodigy scanner (GE Medical Systems). QCT scans of the spine and hip were performed at baseline and again at 36 months using a 128-slice DE scanner (SOMATOM Definition FLASH, Siemens Healthcare, Germany). Figure 1 provides a schematic comparing the energy sources in a SE versus DE CT scanner. The FLASH scanner provides two simultaneous SE scans using the two x-ray sources, one at 100 kVp (tube A) and the other at 140 kVp (tube B). A tin-filter was added to tube B to allow for better separation of the X-ray spectra of the 140 kVp scan from the low kVp scan than in older instruments.[7, 8] Since spectra separation is one of the primary limiting factors influencing the precision of DE QCT, this technique provides much improved precision as compared to previous

scanners. The reason why the 100 kVp was selected as the low kVp instead of traditional 80 kVp in the DE scan was because the 100 kVp allows better penetration of high attenuating body regions, such as pelvis, and thus improves image noise and the precision of QCT results as compared to 80 kVp. The scanning and reconstruction techniques were as follows: rotation time, 0.5 second; detector configuration, 32x0.6 mm; automatic exposure control was on (CAREdose4D, Siemens Healthcare) with the quality reference mAs of 155 for 100 kVp and 120 for 140 kVp; Nominal CTDIvol, 12.3 mGy; reconstruction kernel, D30 with a slice thickness of 2 mm and slice interval of 2 mm. Table height was fixed for all patients. A calibration phantom (Mindways Inc.) was scanned together with the patient to provide the basis for calibration. Images were then analyzed as either SE scans (100 kVp) or DE scans, with the latter accounting for bone marrow fat.

Analysis for vBMD and marrow fat

Details regarding the spine and femur CT scan processing and assessment of vBMD measures from our group have previously been described.[6, 9] For assessment of vBMD and marrow fat, we assume a three-compartmental model consisting of calcium, red marrow (soft tissue) and yellow marrow (fat). With the assumption of volume constraint of the three material composition (calcium or fat would displace certain amount of red marrow), the three-compartmental model can be solved using the DE measurements at the two X-ray energies (100 and 140 kV), which are given by:

$$CT_{ROI}^{100} = k_{Ca}^{100} \rho_{ca} + k_F^{100} \rho_F + \beta^{100} \quad (\text{Eq. 1})$$

$$CT_{ROI}^{140} = k_{Ca}^{140} \rho_{ca} + k_F^{140} \rho_F + \beta^{140} \quad (\text{Eq. 2})$$

where CT_{ROI}^{100} and CT_{ROI}^{140} denote the CT number measurement at a region of interest (ROI) for 100 kVp and 140 kVp, respectively. Coefficients k_{Ca}^{100} , β^{100} , k_{Ca}^{140} , and β^{140} were determined by linear regression using a calibration phantom (QA phantom, Mindways Inc.). Currently there is no consensus on which fat-equivalent material should be used for marrow fat.[10] To improve stability of the dual-energy solution, coefficients k_F^{100} and k_F^{140} were assumed to be the same,[4] which equals to $-0.1 \text{ HU}/(\text{mg}/\text{cc})$ in this work. Using these equations we can solve for ρ_{Ca} as:

$$\rho_{Ca} = \frac{(CT_{ROI}^{140} - \beta^{140}) \cdot k_F^{100} - (CT_{ROI}^{100} - \beta^{100}) \cdot k_F^{140}}{k_{Ca}^{140} \cdot k_F^{100} - k_{Ca}^{100} \cdot k_F^{140}}$$

And ρ_F as:

$$\rho_F = \frac{(CT_{ROI}^{140} - \beta^{140}) \cdot k_{Ca}^{100} - (CT_{ROI}^{100} - \beta^{100}) \cdot k_{Ca}^{140}}{k_F^{140} \cdot k_{Ca}^{100} - k_F^{100} \cdot k_{Ca}^{140}}$$

These values were calculated for each voxel in the region. The calcium concentration for an entire ROI was calculated by averaging the concentration of all the voxels in the ROI. The voxel-by-voxel fat concentration was calculated with a physiologic constraint, which is no less than 0 mg/cc and no more than 600 mg/cc at any voxel, before averaging voxels to obtain the concentration for the ROI. The reason why a constraint was applied to the fat concentration was due to the inherent unstable DE analysis, i.e., a small change of CT number may lead to a large change of fat concentration; thus, a constraint on fat concentration can improve stability. To minimize error due to patient position and operator variation, follow-up scans were rigidly co-registered to the baseline scan at first, and then the concentrations of vBMD and fat were calculated in the same ROIs as the baseline scan.

Biochemical and hormonal measurements

Total 25-hydroxyvitamin D (25-OHD) was measured using liquid chromatography-tandem mass spectrometry (LC-MS/MS; API 5000; Applied Biosystems-MDS Sciex, Foster City, CA; interassay CV, 6.8%). Serum E₂ was measured using LC-MS/MS as previously described[11] (interassay CV, 8%). Follicle stimulating hormone (FSH) was measured by two-site immunoenzymatic assay (Beckman Instruments, Chaska, MN; interassay CV, 3.8%). Intact parathyroid hormone-intact (PTH) was measured by solid phase, two-site immunoassay (Siemens Healthcare Diagnostics, Deerfield, IL interassay CV, 3.3%). Bone formation was assessed by serum amino-terminal propeptide of type I collagen (PINP) as measured by double-antibody radioimmunoassay (DiaSorin, Stillwater, MN; interassay CV, 6.5%). Bone resorption was evaluated by serum cross-linked C-telopeptide of type I collagen (CTX) using an enzyme-linked immunosorbent assay (ELISA, Roche Diagnostics, Indianapolis, IN; interassay CV, 8.0%). Eight women with E₂ values > 20 pg/mL were removed from analyses of the hormonal and bone turnover measures.

Statistical analyses

We assessed the 3-year changes in lumbar spine and femur neck vBMD using both SE QCT and DE QCT analyses. In addition, we also evaluated longitudinal changes in marrow fat in the early menopausal period using DE QCT. Baseline and rate characteristics were summarized using mean \pm standard deviation as well as median and range. Signed rank tests were used to test whether changes differed from 0. The relationships between baseline and annualized rates of change in vBMD and marrow fat variables versus marrow fat and biochemical/hormonal variables were studied using Spearman correlations. Analyses were conducted using SAS 9.4 (SAS Institute, Cary, NC) and R 3.3.1.[12]

Results

Variability and radiation dosimetry of SE versus DE QCT

As noted earlier, one of the concerns regarding DE QCT scanning was the greater variability of measurements with this technique versus SE QCT.[4, 5] Thus, we initially performed repeat L1–L3 vertebral scans on 6 elderly women (age 70–81 years). Using the DE scanner and scanning protocol, coefficients of variation (CVs) for the SE scans were 1.2% versus 1.6% for the DE scans. A further limitation to the widespread use of DE QCT in clinical practice has been the additional radiation dose to subjects compared to standard SE QCT.[4, 5] With the scanning protocol utilized in this study, estimated effective doses for either SE QCT scans (2.6 mSv) or DE QCT scans (5.5 mSv), including both hip and spine scans, were well below those for similar medical procedures (e.g., routine abdomen/pelvis CT, 14.2 mSv; CT colonography, 10.6 mSv). Thus, the DE scanner provides satisfactory CVs and radiation exposure in a generally acceptable range.

Baseline variables

Table 1 shows the baseline characteristics of the study subjects. The women were, on average, ~7 years since menopause (YSM). Median 25-OHD levels were 33.0 ng/mL. Table 2 shows the baseline vBMD variables using either SE or DE QCT as well as the marrow fat values using DE scanning. As is evident, SE QCT substantially underestimated trabecular vBMD at the spine and femur neck (by –17.6% and –13.1%, respectively), with a much smaller difference (–3.2%) for femur neck cortical vBMD. Note, however, that although median values for percent underestimation of vBMD are provided in Table 2, this varied considerably as a function of baseline vBMD. As shown in Figures 2A and B, for both femur neck and lumbar spine trabecular vBMD, the underestimation of vBMD by SE QCT became progressively larger at lower vBMD values. Marrow fat was substantially (~13%) higher at the femur neck as compared to the lumbar spine (Table 2).

Table 3 shows the annualized percent changes in SE and DE QCT vBMD variables as well as in marrow fat at the femur neck and lumbar spine. SE QCT substantially overestimated decreases in trabecular vBMD, by 14.4% and 24.2% at the femur neck and lumbar spine, respectively, with a smaller difference (8.8%) for changes in femur neck cortical vBMD. As shown in Figures 3A and B, annualized changes in femur neck and lumbar spine trabecular vBMD using SE or DE QCT were highly correlated, but as these changes became more negative, the overestimation of the decreases using SE QCT became progressively greater as shown by the greater deviation from the line of identity in the Figures. Marrow fat increased at both the femur neck and lumbar spine, with a >4-fold greater increase at the femur neck compared to the lumbar spine (Table 3).

Table 4 shows the correlations between the baseline and annualized rates of change in SE vBMD versus the marrow fat and biochemical/hormonal variables. Even within this fairly narrow age range, age was negatively correlated with the baseline vBMD variables, except for femur neck cortical vBMD, but not with rates of change in SE vBMD. YSM showed a similar negative correlation with the baseline vBMD variables, but was protective against bone loss at the femur neck cortex, perhaps reflecting the more rapid bone loss early after

menopause. BMI was negatively correlated with baseline femur neck cortical vBMD, but protective against bone loss in the femur neck trabecular compartment. As expected, baseline femur neck and spine marrow fat was negatively correlated with SE trabecular vBMD in these regions, but baseline marrow fat did not predict rates of change in vBMD at either site. Negative correlations between the rate of change in marrow fat at the femur neck and rates of change in trabecular vBMD indicate that greater increases in marrow fat were associated with greater decreases in trabecular vBMD. The biochemical/hormonal variables did not show any consistent relationships to the SE QCT variables.

Table 5 shows the analogous relationships between baseline and annualized rates of change in DE vBMD as well as marrow fat variables and the marrow fat plus biochemical/hormonal variables. Age was a negative predictor of baseline DE vBMD variables and a positive predictor of marrow fat, with generally similar relationships for YSM. BMI was again negatively correlated with DE femur neck cortical vBMD and positively correlated with lumbar spine marrow fat. BMI was protective against bone loss in the femur neck trabecular compartment and also reduced increases in marrow fat. Baseline marrow fat was negatively correlated with femur neck and spine trabecular vBMD. Of the biochemical and hormonal variables, higher estrogen levels reduced rates of increase in femur neck marrow fat.

Discussion

Although previous studies have compared SE versus DE scanning in cadaveric bones,[4, 5] to our knowledge ours is the first study to use a current generation DE scanner to evaluate SE versus DE QCT scanning both cross-sectionally and longitudinally in a substantial cohort of postmenopausal women. Consistent with the previous cadaveric studies,^(4,5) we found that SE scanning significantly underestimates trabecular vBMD as compared to DE QCT (depending on the actual vBMD, by up to 30%, Figure 2), as the latter corrects for effects of bone marrow fat. In addition, SE QCT scanning overestimates rates of bone loss, and this overestimation is progressively greater than the underlying change in SE QCT (Figure 3). In the past, the advantages of marrow fat correction by DE QCT scanning were offset by the greater variability and radiation exposure associated with this technique. However, given the current generation scanners, the variability is now very acceptable for research as well as clinical use and the radiation exposure is in a generally acceptable range. As such, the ability to correct for cross-sectional and longitudinal changes in marrow fat may well outweigh the precision and radiation concerns associated with older scanners, arguing for greater use of DE scanning, particularly in research protocols.

The use of DE QCT scanning may be particularly relevant in the context of anabolic drug therapies for osteoporosis, as these drugs may alter marrow fat composition. Thus, both PTH[13] and romozosumab[14] have been shown to markedly reduce marrow fat in animal models. As depicted in Figure 4, the black line reflecting the relationship between annualized changes in SE versus DE lumbar spine trabecular vBMD is derived based on the normal aging changes in bone marrow fat in our study. If an anabolic drug had no effect on this relationship, then in the example shown, a 20% increase in trabecular vBMD using SE QCT would correspond to only a 15% increase in trabecular vBMD using DE QCT. However, if a drug dramatically altered marrow fat content, it could shift this relationship to

the hypothetical red line in Figure 3, whereby a 20% increase in vBMD by SE QCT would correspond to only a 10% increase by DE QCT. This effect may explain why, for example, 24 months of treatment with teriparatide was found to result in a remarkable 48% increase in lumbar spine trabecular vBMD, but only a 18% increase in areal BMD by DXA[15] (which may be less confounded by marrow fat changes[16]). Clearly, additional studies are needed to directly evaluate the impact that anabolic drugs which alter marrow fat composition have on SE versus DE assessment of trabecular vBMD changes, and the recently available DE scanning technology should allow for such studies.

As expected, marrow fat had less of an impact on cross-sectional and longitudinal measurements of cortical vBMD at the femur neck than on the trabecular measures. In addition, using both SE and DE QCT, we found an inverse association between BMI and cortical vBMD at the femur neck. These findings are consistent with previous observations, [17] confirming a negative effect of obesity on cortical bone, although the underlying mechanisms for this remain unclear. Interestingly, both SE and DE QCT measures of trabecular vBMD at the femur neck and lumbar spine were negatively correlated with marrow fat, consistent with the known inverse association between marrow fat and bone and distinct from any confounding of marrow fat that may be present with the SE QCT measurements.[18, 19] We also found that higher estrogen levels were associated with smaller increases in marrow fat in the femur neck, consistent with previous work from our group showing that estrogen treatment of postmenopausal women prevented increases in marrow fat over one year.[20]

Marrow adipose tissue behaves differently from visceral adipose tissue. In addition to physiologic aging, disorders such as obesity and anorexia nervosa are associated with increased marrow fat. Further, bone marrow stromal cells demonstrate commitment to adipogenesis following exposure to radiation or chemotherapeutic agents.[21, 22] Interestingly, some of these states are also associated with increased rates of bone loss and increased risk of fractures, suggesting that marrow adipose tissue contributes, directly or indirectly, to bone strength.[23–25] This further highlights the importance of accounting for marrow adipose tissue during fracture risk assessment, at least in select populations.

In order to put our findings in the broader context of available imaging technologies for bone, Table 6 summarizes the radiation doses and key features of DXA, SE QCT, DE QCT, and high resolution peripheral QCT (HRpQCT). Each modality has specific advantages and potential disadvantages and which technology is utilized would depend on the specific research or clinical indication. For example, if the goal is to assess bone microarchitecture, then HRpQCT is the preferred modality, but this is only feasible at a peripheral site. Conversely, if the intent is to evaluate trabecular versus cortical bone separately at a central site independent of effects of bone marrow fat, then DE QCT is the preferred option, albeit requiring higher radiation.

Limitations of our study include the lack of a gold standard technique to assess rate of bone loss to which data from both SE QCT and DE QCT could be compared. Such an approach would have required invasive techniques for assessment of bone content, most of which cannot be performed *in vivo*. In addition, we studied women between the ages of 50 to 61

years, and findings may be different in much older women with a greater amount of marrow fat in their bones.

In summary, the advent of current DE scanning technology circumvents previous concerns regarding the precision and radiation exposure associated with this technique, which can correct for cross-sectional and longitudinal changes in bone marrow fat. The effects of marrow fat on SE QCT measurements confound changes associated with normal aging, and may be particularly relevant in the context of anabolic osteoporosis treatments that increase bone mass but also reduce marrow fat. Additional studies are needed to more fully evaluate the potential effects both of aging and drug therapy on SE versus DE QCT changes in vBMD, and these studies should now be feasible using the recently available DE scanning technology.

Acknowledgments

Grant support: NIH AR027065 and UL1TR002377

All authors accept responsibility for the integrity of the data presented in this manuscript. LKM and AJT contributed to data acquisition and final approval of the manuscript. EJA and SJA contributed to the experimental design, data analysis, and final approval of the manuscript. SK, JGS, MTD, JJC, LY, MCA and SA contributed to the experimental design, data interpretation, all drafts and final approval of the manuscript.

References

1. Sheu Y, Cauley JA. The role of bone marrow and visceral fat on bone metabolism. *Curr Osteoporos Rep.* 2011; 9:67–75. [PubMed: 21374105]
2. Engelke K, Adams JE, Armbrecht G, Augat P, Bogado CE, Bouxsein ML, Felsenberg D, Ito M, Prevrhal S, Hans DB, Lewiecki EM. Clinical use of quantitative computed tomography and peripheral quantitative computed tomography in the management of osteoporosis in adults: the 2007 ISCD Official Positions. *J Clin Densitom.* 2008; 11:123–62. [PubMed: 18442757]
3. Wesarg S, Kirschner M, Becker M, Erdt M, Kafchitsas K, Khan MF. Dual-energy CT-based assessment of the trabecular bone in vertebrae. *Methods Inf Med.* 2012; 51:398–405. [PubMed: 23038636]
4. Gluer CC, Reiser UJ, Davis CA, Rutt BK, Genant HK. Vertebral mineral determination by quantitative computed tomography (QCT): accuracy of single and dual energy measurements. *J Comput Assist Tomogr.* 1988; 12:242–258. [PubMed: 3351039]
5. Gluer CC, Genant HK. Impact of marrow fat on accuracy of quantitative CT. *J Comput Assist Tomogr.* 1989; 13:1023–1035. [PubMed: 2584480]
6. Riggs BL, Melton LJ 3rd, Robb RA, Camp JJ, Atkinson EJ, McDaniel L, Amin S, Rouleau PA, Khosla S. A population-based assessment of rates of bone loss at multiple skeletal sites: evidence for substantial trabecular bone loss in young adult women and men. *J Bone Miner Res.* 2008; 23:205–214. [PubMed: 17937534]
7. Johnson TR. Dual-energy CT: general principles. *Am J Roentgenol.* 2012; 199(5 Suppl):S3–8. [PubMed: 23097165]
8. Primak AN, Ramirez Giraldo JC, Liu X, Yu L, McCollough CH. Improved dual-energy material discrimination for dual-source CT by means of additional spectral filtration. *Medical physics.* 2009; 36:1359–69. [PubMed: 19472643]
9. Riggs BL, Melton LJ 3rd, Robb RA, Camp JJ, Atkinson EJ, Peterson JM, Rouleau PA, McCollough CH, Bouxsein ML, Khosla S. Population-based study of age and sex differences in bone volumetric density, size, geometry, and structure at different skeletal sites. *J Bone Miner Res.* 2004; 19:1945–1954. [PubMed: 15537436]

10. Steenbeek JC, van Kuijk C, Grashuis JL, van Panthaleon van Eck RB. Selection of fat-equivalent materials in postprocessing dual-energy quantitative CT. *Medical physics*. 1992; 19:1051–6. [PubMed: 1518467]
11. Khosla S, Amin S, Singh RJ, Atkinson EJ, Melton LJ 3rd, Riggs BL. Comparison of sex steroid measurements in men by immunoassay versus mass spectroscopy and relationships with cortical and trabecular volumetric bone mineral density. *Osteoporos Int*. 2008; 19:1465–1471. [PubMed: 18338096]
12. R.C. Team. R: A language and environment for statistical computing. R Foundation for Statistical Computing; Vienna, Austria: 2016. URL <https://www.R-project.org/>
13. Fan Y, Hanai JI, Le PT, Bi R, Maridas D, DeMambro V, Figueroa CA, Kir S, Zhou X, Mannstadt M, Baron R, Bronson RT, Horowitz MC, Wu JY, Bilezikian JP, Dempster DW, Rosen CJ, Lanske B. Parathyroid Hormone Directs Bone Marrow Mesenchymal Cell Fate. *Cell Metab*. 2017; 25:661–672. [PubMed: 28162969]
14. Fairfield H, Falank C, Harris E, Demambro V, McDonald M, Pettitt JA, Mohanty ST, Croucher P, Kramer I, Kneissel M, Rosen CJ, Reagan MR. The skeletal cell-derived molecule sclerostin drives bone marrow adipogenesis. *Journal of cellular physiology*. 2018; 233:1156–1167. [PubMed: 28460416]
15. Finkelstein JS, Hayes A, Hunzelman JL, Wyland JJ, Lee H, Neer RM. The effects of parathyroid hormone, alendronate, or both in men with osteoporosis. *N Engl J Med*. 2003; 349:1216–1226. [PubMed: 14500805]
16. Kuiper JW, van Kuijk C, Grashuis JL, Ederveen AG, Schutte HE. Accuracy and the influence of marrow fat on quantitative CT and dual-energy X-ray absorptiometry measurements of the femoral neck in vitro. *Osteoporos Int*. 1996; 6:25–30. [PubMed: 8845596]
17. Sukumar D, Schlüssel Y, Riedt CS, Gordon C, Stahl T, Shapses SA. Obesity alters cortical and trabecular bone density and geometry in women. *Osteoporos Int*. 2011; 22:635–45. [PubMed: 20533027]
18. Patsch JM, Li X, Baum T, Yap SP, Karampinos DC, Schwartz AV, Link TM. Bone marrow fat composition as a novel imaging biomarker in postmenopausal women with prevalent fragility fractures. *J Bone Miner Res*. 2013; 28:1721–8. [PubMed: 23558967]
19. Hui SK, Arentsen L, Sueblinvong T, Brown K, Bolan P, Ghebre RG, Downs L, Shanley R, Hansen KE, Minenko AG, Takhashi Y, Yagi M, Zhang Y, Geller M, Reynolds M, Lee CK, Blaes AH, Allen S, Zobel BB, Le C, Froelich J, Rosen C, Yee D. A phase I feasibility study of multi-modality imaging assessing rapid expansion of marrow fat and decreased bone mineral density in cancer patients. *Bone*. 2015; 73:90–7. [PubMed: 25536285]
20. Syed FA, Oursler MJ, Hefferanm TE, Peterson JM, Riggs BL, Khosla S. Effects of estrogen therapy on bone marrow adipocytes in postmenopausal osteoporotic women. *Osteoporos Int*. 2008; 19:1323–1330. [PubMed: 18274695]
21. Sacks EL, Goris ML, Glatstein E, Gilbert E, Kaplan HS. Bone marrow regeneration following large field radiation: influence of volume, age, dose, and time. *Cancer*. 1978; 42:1057–65. [PubMed: 100197]
22. Georgiou KR, Foster BK, Xian CJ. Damage and recovery of the bone marrow microenvironment induced by cancer chemotherapy - potential regulatory role of chemokine CXCL12/receptor CXCR4 signalling. *Curr Mol Med*. 2010; 10:440–53. [PubMed: 20540706]
23. Rosen CJ, Bouxsein ML. Mechanisms of disease: is osteoporosis the obesity of bone? *Nat Clin Pract Rheumatol*. 2006; 2:35–43. [PubMed: 16932650]
24. Bredella MA, Fazeli PK, Miller KK, Misra M, Torriani M, Thomas BJ, Ghomi RH, Rosen CJ, Klibanski A. Increased bone marrow fat in anorexia nervosa. *J Clin Endocrinol Metab*. 2009; 94:2129–36. [PubMed: 19318450]
25. Bredella MA, Gill CM, Gerweck AV, Landa MG, Kumar V, Daley SM, Torriani M, Miller KK. Ectopic and serum lipid levels are positively associated with bone marrow fat in obesity. *Radiology*. 2013; 269:534–41. [PubMed: 23861502]

Highlights

- We used a dual-energy computed tomography scanner to assess volumetric BMD in women
- Single-energy quantitative computed tomography (QCT) substantially underestimated trabecular vBMD at both the spine and femur as compared to dual-energy QCT
- Single-energy QCT also substantially overestimated rates of bone loss in trabecular vBMD as compared to dual-energy QCT
- These findings have implications for evaluation of age-related bone loss and vBMD changes following anabolic therapies that alter marrow fat

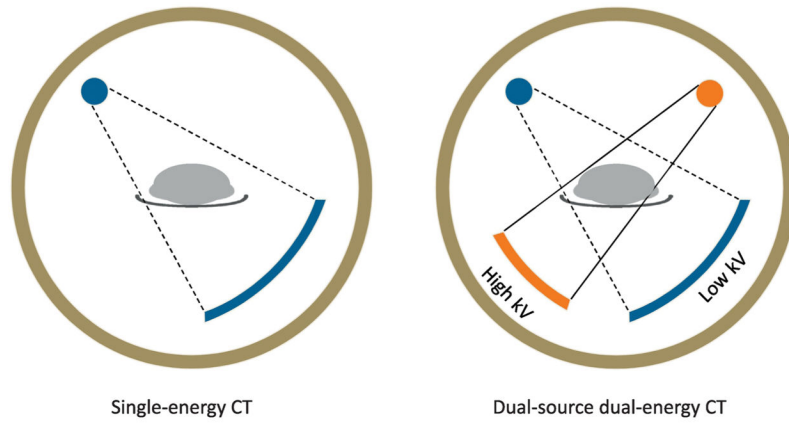


Figure 1. Schematic comparing the energy sources in a SE versus DE CT scanner.

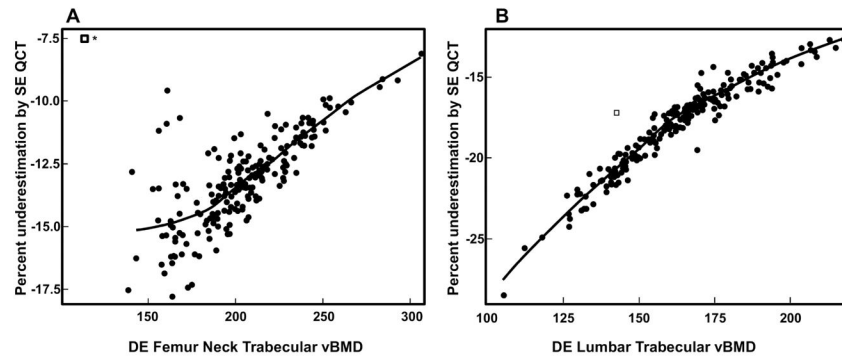


Figure 2. (A) Relationship between DE femur neck trabecular vBMD and the percent underestimation of femur neck trabecular vBMD by SE QCT; (B) Relationship between lumbar spine trabecular vBMD and the percent underestimation of lumbar trabecular vBMD by SE QCT

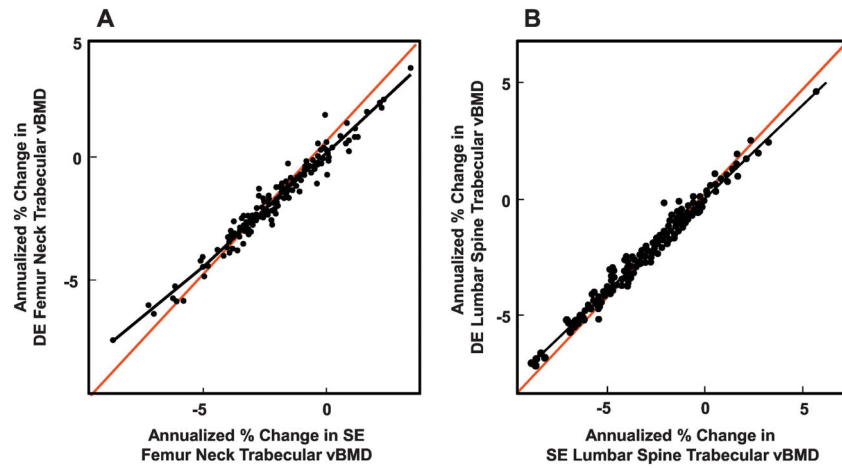


Figure 3.

(A) Annualized percent changes in SE femur neck trabecular vBMD versus annualized percent changes in DE femur neck trabecular vBMD (Spearman $R = 0.97$, $P < 0.001$); (B) Annualized percent changes in lumbar spine trabecular vBMD versus annualized percent changes in DE lumbar spine trabecular vBMD (Spearman $R = 0.99$, $P < 0.001$). Black lines show the actual relationship; red lines are lines of identity.

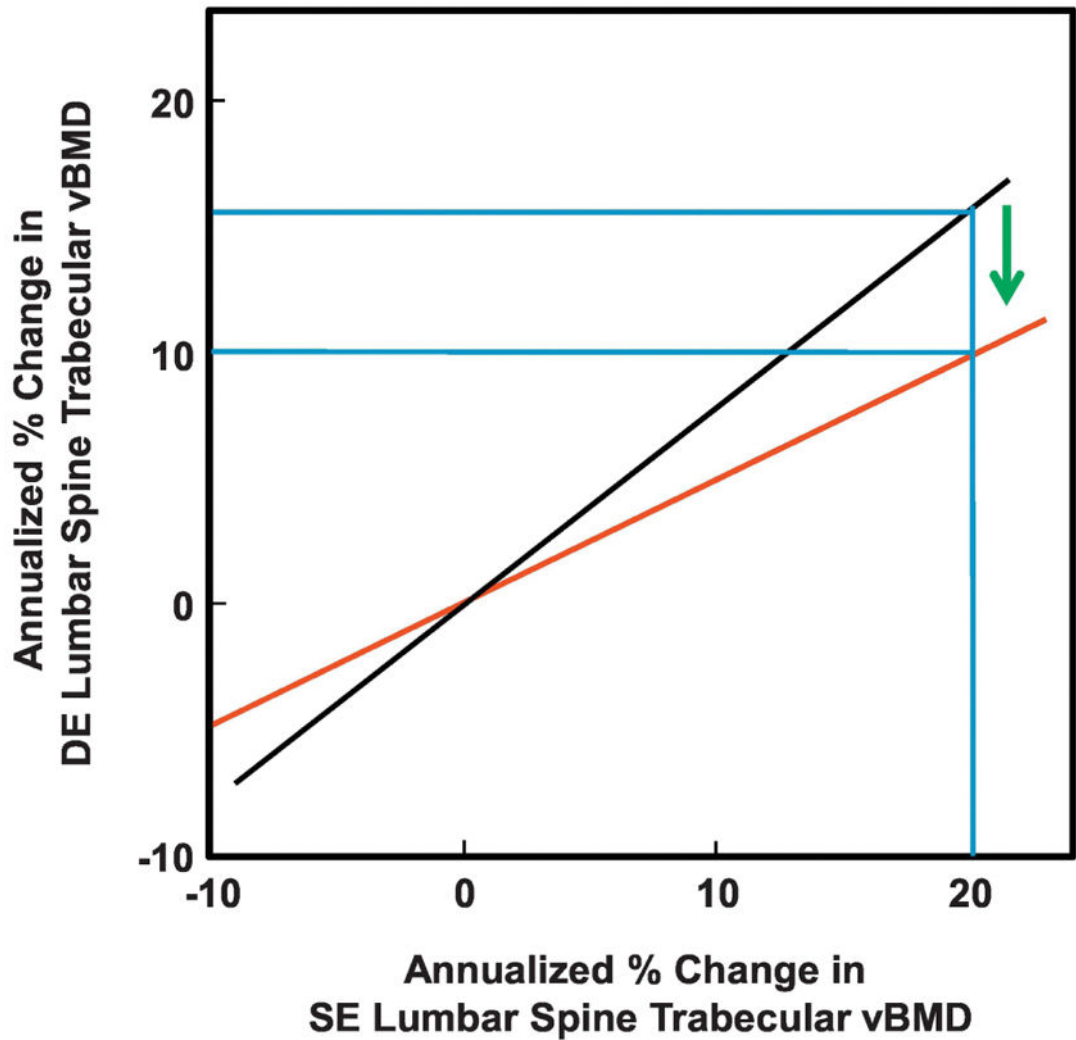


Figure 4. Potential effects of marrow fat on changes in SE versus DE trabecular vBMD following anabolic drugs. Black line shows the actual relationship between SE versus DE spine trabecular vBMD changes from this study. Red line shows a hypothetical relationship for a drug that markedly reduces marrow fat. Please see Discussion for details.

Table 1

Baseline characteristics of the study subjects.

	N	mean ± SD, median (IQR)
Age (years)	197	56.5 ± 2.7 56.7 (54.4, 58.7)
Years since menopause *	177	7.3 ± 5.4 6.0 (3.5, 9.3)
Height (cm)	197	163.7 ± 5.7 163.5 (159.8, 167.9)
Weight (kg)	197	70.2 ± 11.5 69.3 (61.6, 75.7)
BMI (kg/m²)	197	26.2 ± 4.3 25.6 (23.1, 28.7)
25-hydroxyvitamin D (ng/mL)	189	33.5 ± 10.0 33.0 (27.0, 40.0)
Estradiol (pg/mL)	189	3.3 ± 1.9 2.8 (2.1, 4.1)
FSH (IU/L)	189	77.8 ± 30.3 73.2 (57.5, 91.1)
PTH (pg/mL)	189	33.4 ± 17.9 30.0 (22.0, 41.0)
PINP (µg/L)	187	66.8 ± 22.1 63.7 (51.6, 79.9)
CTX (ng/mL)	187	0.56 ± 0.20 0.54 (0.40, 0.70)

* The women whose last menstrual date was the same as the hysterectomy date and did not have an oophorectomy were not summarized for years to menopause.

Baseline vBMD and marrow fat variables [median (IQR)].

Table 2

Parameter	N	SE QCT	DE QCT	Signed Rank Test p-value	% underestimation by SE QCT
Femur Neck					
Total vBMD (mg/cm³)	194	307 (283 – 338)	337 (312 – 369)	<0.001	-8.6 (-9.4, -8.0) [‡]
Cortical vBMD (mg/cm³)	194	594 (567 – 629)	615 (587 – 648)	<0.001	-3.2 (-3.6, -2.8) [‡]
Trabecular vBMD (mg/cm³)	194	176 (158 – 197)	202 (185 – 222)	<0.001	-13.1 (-14.4, -11.9) [‡]
Marrow fat (mg/cm³)	194	n/a	318 (295 – 344)	n/a	
Lumbar spine					
Trabecular vBMD (mg/cm³)	197	134 (116 – 147)	162 (146 – 176)	<0.001	-17.6 (-20.0, -16.0) [‡]
Marrow fat (mg/cm³)	197	n/a	281 (264 – 295)	n/a	

* <0.05,

[†] <0.01,

[‡] <0.001 p-value for signed rank test for change different from 0

Table 3

Annualized percent changes in vBMD and marrow fat variables [median (IQR)].

Parameter	N	SE QCT	DE QCT	Signed Rank Test p-value	% overestimation by SE QCT
Femur Neck					
Total vBMD (mg/cm³)	171	-1.68 (-2.33, -0.99) [‡]	-1.41 (-2.08, -0.82) [‡]	<0.001	+13.1 (5.2, 23.6) [‡]
Cortical vBMD (mg/cm³)	171	-0.96 (-1.70, -0.30) [‡]	-0.88 (-1.52, -0.21) [‡]	<0.001	+8.8 (-7.0, 27.4) [‡]
Trabecular vBMD (mg/cm³)	171	-2.02 (-3.13, -0.94) [‡]	-1.67 (-2.63, -0.75) [‡]	<0.001	+14.4 (1.2, 28.6) [‡]
Marrow fat (mg/cm³)	171	n/a	1.35 (-1.49, 4.66) [‡]	n/a	n/a
Lumbar spine					
Trabecular vBMD (mg/cm³)	176	-2.05 (-3.26, -0.96) [‡]	-1.69 (-2.59, -0.63) [‡]	<0.001	+24.2 (15.1, 33.8) [‡]
Marrow fat (mg/cm³)	176	n/a	0.31 (-1.00, 2.32) [‡]	n/a	

* <0.05,

[‡] <0.01,

[‡] <0.001 p-value for signed rank test for change different from 0

Table 4

Correlations between baseline and annualized rates of change in SE vBMD versus the marrow fat and biochemical/hormonal variables.

	Age	YSM	BMI	DE baseline femur marrow fat	DE baseline spine marrow fat	DE change in femur marrow fat	DE change in spine marrow fat	25-OHD	E2	FSH	PTH	PINP	CTX
SE Baseline values													
Femur Neck													
Total vBMD (mg/cm ³)	-0.26 [‡]	-0.21 [‡]	-0.12	-0.33 [‡]	-0.06	0.16 [*]	-0.01	-0.05	-0.02	-0.03	-0.05	0.12	0.02
Cortical vBMD (mg/cm ³)	-0.06	-0.09	-0.26 [‡]	-0.02	0.00	0.20 [‡]	0.00	0.01	-0.08	-0.07	-0.12	0.03	0.00
Trabecular vBMD (mg/cm ³)	-0.32 [‡]	-0.27 [‡]	-0.09	-0.48 [‡]	-0.15 [*]	0.14	0.04	-0.05	-0.06	0.07	0.00	0.16 [*]	0.06
Lumbar spine													
Trabecular vBMD (mg/cm ³)	-0.28 [‡]	-0.32 [‡]	-0.12	-0.28 [‡]	-0.57 [‡]	0.07	0.15 [*]	-0.02	-0.08	0.17 [*]	0.11	0.07	0.05
SE Annualized rates of change													
Femur Neck													
Total vBMD (mg/cm ³)	0.05	0.19 [*]	0.13	0.14	0.14	-0.09	-0.05	-0.07	0.15	0.03	-0.08	0.10	-0.05
Cortical vBMD (mg/cm ³)	0.14	0.16 [*]	0.04	0.07	0.13	0.00	-0.10	0.04	0.09	0.06	-0.11	-0.09	-0.12
Trabecular vBMD (mg/cm ³)	0.04	0.12	0.15 [*]	0.10	0.13	-0.18 [*]	-0.09	-0.09	0.09	0.03	-0.03	0.15 [*]	0.04
Lumbar spine													
Trabecular vBMD (mg/cm ³)	-0.03	0.08	0.06	0.13	0.10	-0.21 [‡]	-0.14	0.02	0.08	-0.02	0.00	-0.08	-0.13

* <0.05,

[‡] <0.01,

^{‡‡} <0.001.

Table 5

Correlations between baseline and annualized rates of change in DE vBMD and marrow fat variables versus the marrow fat and biochemical/hormonal variables.

	Age	YSM	BMI	Baseline femur marrow fat	Baseline spine marrow fat	Change in femur marrow fat	Change in spine marrow fat	25-OHD	E2	FSH	PTH	PINP	CTX
DE Baseline values													
Femur Neck													
Total vBMD (mg/cm ³)	-0.26[‡]	-0.21[‡]	-0.11	-0.33[‡]	-0.06	0.14	-0.02	-0.06	-0.01	-0.03	-0.06	0.12	0.02
Cortical vBMD (mg/cm ³)	-0.07	-0.10	-0.22[‡]	-0.04	0.00	0.20[‡]	-0.01	-0.00	-0.06	-0.08	-0.10	0.02	-0.00
Trabecular vBMD (mg/cm ³)	-0.32[‡]	-0.27[‡]	-0.09	-0.47[‡]	-0.15[*]	0.13	0.04	-0.05	-0.06	0.07	-0.00	0.16[*]	0.07
Marrow fat (mg/cm ³)	0.19[‡]	0.12	-0.07	--	0.17[*]	-0.38[‡]	-0.08	0.12	0.00	-0.03	-0.09	-0.05	-0.07
Lumbar spine													
Trabecular vBMD (mg/cm ³)	-0.29[‡]	-0.32[‡]	-0.10	-0.29[‡]	-0.56[‡]	0.07	0.15	-0.02	-0.07	0.16[*]	0.11	0.07	0.04
Marrow fat (mg/cm ³)	0.21[‡]	0.32[‡]	0.25[‡]	0.17[*]	--	-0.01	-0.42[‡]	0.04	0.12	-0.10	-0.10	-0.01	-0.03
DE Annualized rates of change													
Femur Neck													
Total vBMD (mg/cm ³)	0.07	0.20[*]	0.16[*]	0.13	0.16[*]	-0.05	-0.05	-0.07	0.15	0.00	-0.05	0.09	-0.05
Cortical vBMD (mg/cm ³)	0.15	0.15	0.06	0.09	0.13	0.02	-0.10	0.02	0.08	0.07	-0.06	-0.09	-0.13
Trabecular vBMD (mg/cm ³)	0.05	0.10	0.16[*]	0.04	0.14	-0.07	-0.07	-0.08	0.10	0.02	-0.00	0.17[*]	0.06
Marrow fat (units)	-0.09	-0.19[*]	-0.18[*]	-0.38[‡]	-0.01	--	0.14	0.03	-0.22[‡]	0.16[*]	-0.01	0.06	0.13
Lumbar spine													
Trabecular vBMD (mg/cm ³)	-0.00	0.09	0.05	0.14	0.10	-0.19[*]	-0.07	0.00	0.09	-0.03	-0.00	-0.07	-0.13
Marrow fat (mg/cm ³)	-0.05	-0.00	-0.13	-0.08	-0.42[‡]	0.14	--	0.04	-0.09	0.02	0.05	0.11	0.13

* <0.05,

‡ <0.01,

‡ <0.001.

Table 6

Summary of radiation doses and key features of different bone imaging technologies.

	Radiation exposure	Advantages	Disadvantages
DXA	0.02 mSv	<ul style="list-style-type: none"> • Low radiation dose • Extensive clinical data/validation 	<ul style="list-style-type: none"> • Cannot separate trabecular versus cortical bone • Areal BMD, so influenced by bone size
SE QCT	2.6 mSv	<ul style="list-style-type: none"> • Can separate trabecular versus cortical bone • Volumetric BMD, so independent of bone size 	<ul style="list-style-type: none"> • Higher radiation dose than DXA • Influenced by bone marrow fat
DE QCT	5.5 mSv	<ul style="list-style-type: none"> • Can separate trabecular versus cortical bone • Volumetric BMD, so independent of bone size • Not confounded by bone marrow fat 	<ul style="list-style-type: none"> • Higher radiation dose than SE QCT
HRpQCT	0.005 mSv	<ul style="list-style-type: none"> • Low systemic radiation • Can separate trabecular versus cortical bone • Allows for assessment of bone microarchitecture 	<ul style="list-style-type: none"> • Can only be done at peripheral sites (radius and tibia)